Progress In Electromagnetics Research B, Vol. 37, 1–19, 2012

EXPONENTIAL DECAY OF HIGH-ORDER SPURIOUS PROLATE SPHEROIDAL MODES INDUCED BY A LOCAL APPROXIMATE DtN EXTERIOR BOUNDARY CONDITION

H. Barucq[1, 2], R. Djellouli[3, *], and A. Saint-Guirons[4]

[1]INRIA Bordeaux Sud-Ouest Research Center Team-Project Magique3D, Université de Pau et des Pays de l'Adour, IPRA-Avenue de l'Université, 64013 Pau, France

[2]Laboratoire de Mathématiques et leurs Applications, CNRS UMR 5142, Université de Pau et des Pays de l'Adour, IPRA-Avenue de l'Université, 64013 Pau, France

[3]Department of Mathematics, California State University Northridge, & Interdisciplinary Research Institute for the Sciences, IRIS, USA

[4]Basque Center of Applied Mathematics (BCAM), Bizkaia Technology Park, Building 500, 48160 Derio, Basque Country, Spain

Abstract—We investigate analytically the asymptotic behavior of high-order spurious prolate spheroidal modes induced by a second-order local approximate DtN absorbing boundary condition (DtN2) when employed for solving high-frequency acoustic scattering problems. We prove that these reflected modes decay exponentially in the high frequency regime. This theoretical result demonstrates the great potential of the considered absorbing boundary condition for solving efficiently exterior high-frequency Helmholtz problems. In addition, this exponential decay proves the superiority of DtN2 over the widely used Bayliss-Gunsburger-Turkel absorbing boundary condition.

1. INTRODUCTION

A prerequisite step for solving numerically exterior Helmholtz problems using a domain-based formulation such as finite element methods (FEM) or finite difference methods (FDM) is the reformulation of this class of problems in a bounded domain. This is often accomplished

Received 7 October 2011, Accepted 25 November 2011, Scheduled 30 November 2011

* Corresponding author: Rabia Djellouli (rabia.djellouli@csun.edu).

by surrounding the given scatterer(s) (or radiator) by an artificial boundary that is located at some distance (measured in multiples of wavelength of interest) from its surface. A so-called "absorbing" boundary condition is then prescribed on the artificial boundary to represent the "far-field" behavior of the scattered field. The main difficulty here is the design of a simple (in terms of implementation in a FEM code), reliable, and cost-effective boundary condition able to "mimic" the far-field behavior of the scattered. Clearly, the efficiency of such a boundary condition has a tremendous impact on the accuracy, the computational complexity, as well as on the cost-effectiveness of any solution methodology for this class of wave problems that are very important to many applications such as sonar, radar, geophysical exploration, nondestructive testing, etc.. Given that, various absorbing boundary conditions have been designed for over half a century, and the quest for such conditions is still ongoing (see, e.g., the review by Turkel in [20] and the references therein).

Recently, the authors proposed a new absorbing boundary condition based on a local approximation of the Dirichlet-to-Neumann (DtN) operator [3, 17]. This condition distinguishes itself from existing absorbing boundary conditions in many aspects. First, the new local *second-order* approximate DtN boundary condition, denoted by DtN2, is particularly well adapted for elongated scatterers (e.g., submarines) which is not the case for the standard approximate DtN boundary condition [10, 12]. Indeed, the latter condition requires the shape of the artificial boundary to be circular/spherical, and therefore often leads to larger than needed computational domains, which hampers computational efficiency. Second, the new DtN2 boundary condition is exact for the first two modes, easy to implement and to parallelize, and more importantly compatible with the local structure of the computational finite element scheme. The results pertaining to the performance analysis of the proposed DtN2 boundary condition in the *low* frequency regime reported in [3, 17], revealed that DtN2 is (a) very accurate regardless of the slenderness of the boundary of the computational domain, and (b) outperforms the widely-used second-order Bayliss-Gunzbürger-Turkel (BGT2) absorbing boundary condition [5] when expressed in prolate spheroidal coordinates [15, 16]. The situation is similar in the high-frequency regime, as indicated by the results of both the numerical and the analytical investigations reported in [4]. Nevertheless, it has been demonstrated that DtN2 produces reflected prolate spheroidal modes at the exterior boundary. However, it has been established that these spurious modes decay-fortunately-faster than $1/(ka)^{15/8}$ (where k is the wavenumber and a the semi-major axis of the prolate spheroidal-shaped scatterer) [4].

The purpose of this work is to conduct an analytical study of the behavior of the high-order spurious modes induced by the new DtN2 boundary condition, and to establish a sharper estimate that provides a better understanding on their asymptotic behavior in the high-frequency regime. We prove that *all* the high-order reflected prolate spheroidal modes (whether they are propagating, evanescent, or grazing modes) decay — in fact — exponentially as ka tends to ∞. This result is very important to the performance of this absorbing boundary condition since it shows that the effect of these spurious waves on the accuracy level — if any — is negligible in the high frequency regime. Hence, this result provides practitioners with the needed confidence to employ the proposed boundary condition on artificial boundaries that are "close" to the considered scatterer's boundary, leading therefore to small computational domains. Note that the situation is not the same in the case of the standard DtN2/BGT2 boundary conditions (recall that in 3D, the standard DtN2 and BGT2 conditions coincide [11]). More specifically, in the high-frequency regime, the high-order spurious modes (whether they are propagating, evanescent, or grazing modes) created by the standard BGT2/DtN2 boundary condition do not decay, as observed in [2], requiring therefore to place the artificial boundary very far from the obstacle to avoid the deterioration of the accuracy level due to the possible contamination of these non physical modes. Consequently, the present study demonstrates analytically the superiority of the new DtN2 boundary condition designed for prolate spheroidal boundaries over the standard BGT2/DTN2 boundary condition. Recall that previous numerical studies [3, 4, 17] have already indicated that the new DtN2 boundary condition outperforms the standard BGT2/DTN2 boundary condition. Hence, this study suggests DtN2 to be the primary absorbing boundary condition to be employed when solving high-frequency acoustic scattering problems by elongated scatterers. Note that the suggested boundary condition can also be used in the case of two-dimensional scattering problems by electromagnetic waves since such problems can be formulated using the Helmholtz equation, the Dirichlet (resp. Neumann) boundary condition on the scatterer(s) for the scattered field with E-polarization (resp. H-polarization), and the Sommerfeld condition [6].

The remainder of this paper is as follows. First, we specify in Section 2 the nomenclature and assumptions, and formulate the considered three-dimensional acoustic scattering problem in a bounded domain using the new local approximate DtN2 absorbing boundary condition proposed in [3, 17]. Then, we announce in Section 3 the main result of this paper. Section 4 is devoted to the proof of the

result. It is based on three steps, each step is formulated as a Lemma. Concluding remarks are presented in Section 5. Appendix A dedicated to the classification of the prolate spheroidal modes is included only for completeness.

2. PRELIMINARIES

2.1. Notations

Throughout this paper, we use the prolate spheroidal coordinates (ξ, φ, θ) related to the cartesian coordinates (x, y, z) by:

$$x = b\sin\varphi\cos\theta, \quad y = b\sin\varphi\sin\theta \quad \text{and} \quad z = a\cos\varphi$$

where $\varphi \in [0, \pi)$ and $\theta \in [0, 2\pi)$. The parameters a and b are respectively the semi-major and the semi-minor axes of the considered prolate spheroid, and are given by $a = f\cosh\xi$ and $b = f\sinh\xi$ where ξ is strictly positive and the real number f is called the interfocal distance ($f = \sqrt{a^2 - b^2}$). In addition, we adopt the following notations:

- Ω is a prolate spheroidal-shaped scatterer whose surface is denoted by Γ. Ω^e is the open complement in $\mathbb{R}^3$ of the domain $\overline{\Omega}$.
- a_Γ (resp. b_Γ) represents the semi-major (resp. semi-minor) axis of the scatterer Ω, and e_Γ its eccentricity.
- Σ is an artificial boundary surrounding the scatterer Ω. Σ is assumed to be a prolate-spheroid surface.
- a_Σ (resp. b_Σ) is the semi-major (resp. semi-minor) axis of the prolate spheroidal-shaped domain whose exterior surface is Σ with an eccentricity denoted by e_Σ.
- Ω^b is a bounded computational domain whose interior (resp. exterior) boundary is Γ (resp. Σ), as illustrated in Figure 1.
- Δ_Σ is the Laplace Beltrami operator on the artificial boundary Σ.
- k is a positive number representing the wavenumber.
- $R^{(j)}_{mn}(kf, \cosh\xi)$ is the radial spheroidal wave function of the jth kind corresponding to the (mn)th mode (see Chapter 4 in [9]) where $(m, n) \in \mathbb{N}^2$ such that $n \geq m$.
- $S_{mn}(kf, \cos\varphi)$ is the angular spheroidal wave function corresponding to the (mn)th mode (see Chapter 3 in [9]).
- N_{mn} is the normalization factor associated to $S_{mn}(kf, \cos\varphi)$. N_{mn} is given by (see Equation (3.1.32) p. 22 in [9]):

$$N_{mn} = \int_{-1}^{1} [S_{mn}(kf, v)]^2\, dv \tag{1}$$

- λ_{mn} is the prolate spheroidal eigenvalue associated to the (mn)th mode (see p. 11 in [9]).
- For a function F_{mn}, we denote its restriction on Γ by:
$$F_{mn_{|\Gamma}} = F_{mn}\left(e_\Gamma k a_\Gamma, e_\Gamma^{-1}\right) \tag{2}$$
Similarly, the restriction of F_{mn} on Σ is denoted by:
$$F_{mn_{|\Sigma}} = F_{mn}\left(e_\Sigma k a_\Sigma, e_\Sigma^{-1}\right) \tag{3}$$
- The partial derivative of the radial spheroidal wave function $R_{mn}^{(j)}$ with respect to the variable ξ is denoted by $R_{mn}^{(j)'}$, i.e.,
$$R_{mn}^{(j)'} = \frac{\partial R_{mn}^{(j)}}{\partial \xi}; \quad j =\in \mathbb{N} \tag{4}$$
- $r_{mn|_\Sigma}$ are complex numbers given by:
$$r_{mn_{|\Sigma}} = \frac{R_{mn_{|\Sigma}}^{(3)'}}{R_{mn_{|\Sigma}}^{(3)}} \tag{5}$$
- $r_{mn_{|\Sigma}}^{(j)}$ are complex numbers given by:
$$r_{mn_{|\Sigma}}^{(j)} = \begin{cases} \frac{R_{mn_{|\Sigma}}^{(3)'}}{R_{mn_{|\Sigma}}^{(3)}} & \text{if} \quad j = 3 \\ \frac{R_{mn_{|\Sigma}}^{(4)'}}{R_{mn_{|\Sigma}}^{(4)}} & \text{if} \quad j = 4 \end{cases} \tag{6}$$
Note that it follows from (5) and (6) that $r_{mn_{|\Sigma}}^{(3)} = r_{mn_{|\Sigma}}$.
- $\Gamma(\cdot)$ denotes the Gamma function (see, for example, Chapter 6 in [1]).
- $||\cdot||_2$ is the euclidean norm.

2.2. The Acoustic Scattering Problem

We recall that the direct acoustic scattering problem by a rigid sound-soft scatterer Ω can be formulated as follows [7]:

$$\begin{cases} \Delta u^{\text{scat}} + k^2 u^{\text{scat}} = 0 & \text{in } \Omega^e \\ u^{\text{scat}} = -u^{\text{inc}} & \text{on } \Gamma \\ \lim\limits_{||x||_2 \to +\infty} ||x||_2 \left[\frac{\partial u^{\text{scat}}}{\partial ||x||_2} - iku^{\text{scat}}\right] = 0 & \end{cases} \tag{7}$$

where Δ is the Laplace operator, u^{scat} is the scattered field, and u^{inc} is the incident plane wave. Note that u^{inc} can be expressed in prolate

spheroidal coordinates as an infinite series (see Equation (84) p. 386 in [18]):

$$u^{\text{inc}} = \sum_{m=0}^{+\infty} \sum_{n=m}^{+\infty} d_{mn}^{\text{inc}} u_{mn}^{(1)} \left(kf, \cosh\xi, \cos\varphi\right) \tag{8}$$

where the mnth Fourier mode $u_{mn}^{(j)}$ ($j = 1, 3, 4$) is given by:

$$u_{mn}^{(j)} \left(kf, \cosh\xi, \cos\varphi\right) = R_{mn}^{(j)} \left(kf, \cosh\xi\right) \frac{S_{mn}\left(kf, \cos\varphi\right)}{\sqrt{N_{mn}}} \cos m\theta \tag{9}$$

and the mnth Fourier coefficient d_{mn}^{inc} is given by:

$$d_{mn}^{\text{inc}} = 2\varepsilon_m \frac{\mathrm{i}^n}{\sqrt{N_{mn}}} S_{mn}\left(kf, \cos\varphi_0\right) \tag{10}$$

φ_0 being the incident angle of the plane wave u^{inc}, $\varepsilon_m = (2 - \delta_{0m})$, and δ_{0m} is the Kronecker delta symbol.

Furthermore, since the scatterer Ω is assumed to be prolate spheroid, the solution u^{scat} of the exterior boundary value problem (7) is also expressed as an infinite series (see Equation (11.36) p. 422 in [6]):

$$u^{\text{scat}} = \sum_{m=0}^{+\infty} \sum_{n=m}^{+\infty} d_{mn}^{\text{scat}} u_{mn}^{(3)} \left(kf, \cosh\xi, \cos\varphi\right) \tag{11}$$

where the mnth Fourier outgoing mode $u_{mn}^{(3)}(kf, \cosh\xi, \cos\varphi)$ is given by Equation (9) for $j = 3$, whereas the associated mnth Fourier coefficient d_{mn}^{scat} is given by:

$$d_{mn}^{\text{scat}} = -2\varepsilon_m \frac{\mathrm{i}^n}{\sqrt{N_{mn}}} \frac{R_{mn_{|\Gamma}}^{(1)}}{R_{mn_{|\Gamma}}^{(3)}} S_{mn}\left(e_\Gamma k a_\Gamma, \cos\varphi_0\right) \tag{12}$$

Observe that it follows from substituting Equation (10) into Equation (12) that:

$$d_{mn}^{\text{scat}} = -\frac{R_{mn_{|\Gamma}}^{(1)}}{R_{mn_{|\Gamma}}^{(3)}} d_{mn_{|\Gamma}}^{\text{inc}} \tag{13}$$

Note that the Dirichlet boundary condition characterizing the sound-soft nature of the considered scatterer is adopted here for the simplicity of the presentation. The present study and the obtained results can easily be extended to other admissible boundary conditions.

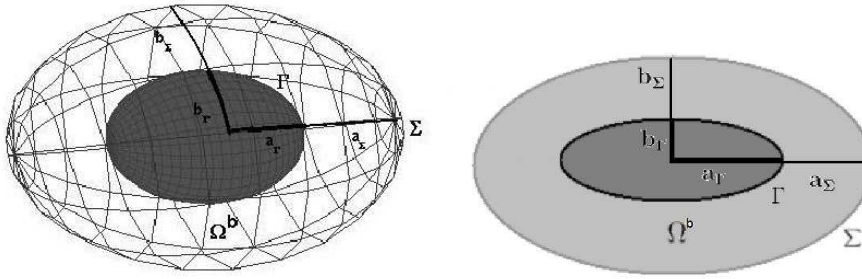

(a) (b)

Figure 1. (a) The bounded computational domain Ω^b with (b) a two-dimensional illustration in the xy-plane.

2.3. Bounded Domain-based Formulation

We reformulate the exterior boundary value problem (7) in a bounded domain Ω^b by surrounding the scatterer Ω with an artificial boundary Σ (see Figure 1), and then by prescribing the new DtN2 absorbing boundary condition suggested in [3, 17] on the exterior boundary Σ. Consequently, the resulting boundary value problem is given by:

$$\begin{cases} \Delta u^{\mathrm{DtN}} + k^2 u^{\mathrm{DtN}} = 0 & \text{in } \Omega^b \\ u^{\mathrm{DtN}} = -u^{\mathrm{inc}} & \text{on } \Gamma \\ \frac{\partial u^{\mathrm{DtN}}}{\partial \mathbf{n}} = \frac{1}{a_\Sigma \sqrt{1-e_\Sigma^2 \cos^2\varphi}} T u^{\mathrm{DtN}} & \text{on } \Sigma \end{cases} \tag{14}$$

where $\mathbf{n}$ is the outward normal to the exterior boundary Σ, and T is the constructed second-order local approximate DtN operator. The differential-type operator T is given by [3, 17]:

$$\begin{aligned} T u^{\mathrm{DtN}} \;=\; & \frac{\sqrt{1-e_\Sigma^2}}{\left(\lambda_{01_{|\Sigma}} - \lambda_{00_{|\Sigma}}\right) e_\Sigma} \Big\{ \Big[\lambda_{01_{|\Sigma}} r_{01_{|\Sigma}} - \lambda_{00_{|\Sigma}} r_{00_{|\Sigma}} \\ & - \left(r_{00_{|\Sigma}} - r_{01_{|\Sigma}} \right) \left(e_\Sigma k a_\Sigma \right)^2 \cos^2\varphi \Big] u^{\mathrm{DtN}} \\ & + \left(r_{00_{|\Sigma}} - r_{01_{|\Sigma}} \right) \Delta_\Sigma u^{\mathrm{DtN}} \Big\} \end{aligned} \tag{15}$$

Note that the field u^{DtN} is an *approximation* of the exact scattered field u^{scat}.

The approximate scattered field u^{DtN} can also be expressed as an infinite series. However, unlike the exact scattered field u^{scat}, this approximate field is a superposition of outgoing modes

$R^{(3)}_{mn}(kf, \cosh\xi))$ and incoming modes $R^{(4)}_{mn}(kf, \cosh\xi))$. More specifically, we have (see Equation (16) p. 233 in [14]):

$$u^{\mathrm{DtN}} = \sum_{m=0}^{+\infty}\sum_{n=m}^{+\infty}\Big[d^{\mathrm{DtN}}_{mn}u^{(3)}_{mn}\left(kf, \cosh\xi, \cos\varphi\right) + \tau^{\mathrm{DtN}}_{mn}u^{(4)}_{mn}\left(kf, \cosh\xi, \cos\varphi\right)\Big] \tag{16}$$

where $u^{(j)}_{mn}(kf, \cosh\xi, \cos\varphi)$ $(j = 3,\ 4)$ is given by Equation (9).

Observe that the incoming modes are spurious waves due to the reflections of the outgoing scattered field at the artificial exterior boundary Σ. In the absence of Σ or in the case of a perfectly nonreflecting boundary condition, the Fourier coefficients satisfy $\tau^{\mathrm{DtN}}_{mn} = 0$ and $d^{\mathrm{DtN}}_{mn} = d^{\mathrm{scat}}_{mn}$ for all $(m, n) \in \mathbb{N}^2$ such that $n \geq m$. Therefore, the degree of transparency of this absorbing boundary condition, and thus the level of accuracy in the approximation as well as the computational cost, depend on (a) the magnitude of the coefficients $|\tau^{\mathrm{DtN}}_{mn}|$ of the reflected waves, and (b) the magnitude of the difference $|d^{\mathrm{DtN}}_{mn} - d^{\mathrm{scat}}_{mn}|$. These two quantities become very small (resp. very large) as the intensity of the reflected waves at the boundary Σ are negligible (resp. very important).

Furthermore, the Fourier coefficients of the solution u^{DtN} satisfy (see Theorem 3.1, p. 588 in [4]):

$$\begin{cases} d^{\mathrm{DtN}}_{mn} = -\dfrac{\Psi^{(4)}_{mn_{|\Sigma}}R^{(1)}_{mn_{|\Gamma}}}{W^{3,4}_{mn}(\Gamma,\Sigma)}d^{\mathrm{inc}}_{mn} \\ \tau^{\mathrm{DtN}}_{mn} = \dfrac{\Psi^{(3)}_{mn_{|\Sigma}}R^{(1)}_{mn_{|\Gamma}}}{W^{3,4}_{mn}(\Gamma,\Sigma)}d^{\mathrm{inc}}_{mn} \end{cases} \tag{17}$$

where d^{inc}_{mn} is given by Equation (10) whereas the function $\Psi^{(j)}_{mn_{|\Sigma}}$ $(j = 3,\ 4)$ is given by:

$$\Psi^{(j)}_{mn|_\Sigma} = R^{(j)}_{mn|_\Sigma}\left[c_{mn|_\Sigma} + r^{(j)}_{mn|_\Sigma}\right] \tag{18}$$

and the functions $R^{(j)}_{mn|_\Sigma}$ and $r^{(j)}_{mn|_\Sigma}$ are defined in Section 2. Moreover, $c_{mn|_\Sigma}$ is given by:

$$c_{mn|_\Sigma} = \frac{r_{00|_\Sigma}\left(\lambda_{01|_\Sigma} - \lambda_{mn|_\Sigma}\right) - r_{01|_\Sigma}\left(\lambda_{00|_\Sigma} - \lambda_{mn|_\Sigma}\right)}{\lambda_{00|_\Sigma} - \lambda_{01|_\Sigma}} \tag{19}$$

Last, the Wronskian-like expression $W^{3,4}_{mn}(\Gamma, \Sigma)$ is given by:

$$W^{3,4}_{mn}(\Gamma, \Sigma) = R^{(3)}_{mn_{|\Gamma}}\Psi^{(4)}_{mn|_\Sigma} - R^{(4)}_{mn_{|\Gamma}}\Psi^{(3)}_{mn|_\Sigma} \tag{20}$$

3. ANNOUNCEMENT OF THE MAIN RESULT

From now on, we assume that the semi-major and semi-minor axes satisfy respectively $a_\Sigma = \sigma a_\Gamma$ and $b_\Sigma = \sigma b_\Gamma$. The positive real number σ, called the widening coefficient, satisfies $\sigma > 1$. Such an assumption implies that the two boundaries have the same eccentricity ($e_\Sigma = e_\Gamma = e$). Note that $\sigma = 1$ corresponds to the extreme case scenario where $\Sigma \equiv \Gamma$, the OSRC formulation [3, 13]. The following result describes the asymptotic behavior of the Fourier coefficient τ_{mn}^{DtN} corresponding to the high-order spurious modes $u_{mn}^{(4)}$. We have:

Theorem 3.1 *For all $(m,n) \in \mathcal{N}$ such that $n \sim \sigma k a_\Gamma$ and $m \leq n$, the reflection Fourier coefficients τ_{mn}^{DtN} given by Equation (17) satisfy:*

$$\left|\tau_{mn}^{\mathrm{DtN}}\right| < 2\kappa \left(\frac{\sqrt{e_\Gamma k a_\Gamma}}{\pi}\right)^{1/4} \exp\left(-\frac{4}{3}\sigma k a_\Gamma \zeta^{3/2}\right); \text{ as } k a_\Gamma \to \infty \quad (21)$$

where $\kappa \approx 1.086435$ and the real number ζ satisfies

$$\frac{2}{3}\zeta^{2/3} = \ln\left[\sigma\left(1 + \sqrt{1-\sigma^{-2}}\right)\right] - \sqrt{1-\sigma^{-2}} \quad (22)$$

The following observations are noteworthy:

i. The asymptotic estimate given by (21) indicates that the high-order spurious modes decay exponentially in the high-frequency regime. This mathematical result proves that the effect of these spurious waves on the accuracy level of the approximation of the scattered field is negligible in the high frequency regime. Consequently, this result provides practitioners with the needed confidence to employ the proposed boundary condition on artificial boundaries that are "close" to the considered scatterer's boundary, leading therefore to small computational domains. Recall that a large computational domain may lead to a prohibitive computational cost since the accuracy requires a very fine mesh in the high frequency regime.

ii. Theorem 3.1 demonstrates the superiority of the new DtN2 absorbing boundary condition given by (15) over the standard DtN2/BGT2 absorbing boundary. Indeed, in the high-frequency regime, the high-order spurious modes (propagating, evanescent, or grazing modes) induced by the standard BGT2/DtN2 boundary condition do not decay, as observed in [2]. Consequently, the use of this condition requires placing the artificial boundary very far from the obstacle in order to avoid the deterioration of the accuracy level due to the presence of the non physical incoming waves. We must point out that previous numerical studies [3, 4, 17] have

already suggested that the new DtN2 boundary condition clearly outperforms the standard BGT2/DTN2 boundary condition.

iii. Theorem 3.1 addresses the asymptotic behavior of the high-modes of the reflected parts of the field u^{DtN}, that is the modes u_{mn} such that $n \sim \sigma k a_\Gamma$ and $m \leq n$. The modes classification presented in Appendix A shows that these modes are of three types: propagating, evanescent, and grazing modes.

4. PROOF OF THEOREM 3.1

This section is devoted to the proof of Theorem 3.1. To this end, we proceed into three steps, each step is formulated as a Lemma.

The first result describes the asymptotic behavior of the functions $\Psi^{(3)}_{mn|_\Sigma}$ given by (18).

Lemma 4.1 *For all $(m,n) \in \mathbb{N}^2$ such that $n \sim \sigma k a_\Gamma$ and $m \leq n$ and, the function $\Psi^{(3)}_{mn|_\Sigma}$ satisfies:*

$$\Psi^{(3)}_{mn|_\Sigma} \sim \frac{\pi^{1/2} 2^{5/6} e_\Gamma \exp(-i\pi 5/6)}{3^{2/3}\Gamma(2/3)} (\sigma k a_\Gamma)^{1/6}\,;\ \text{as } k a_\Gamma \to +\infty \tag{23}$$

Proof of Lemma 4.1. Since the function $\Psi^{(3)}_{mn|_\Sigma}$ is given by Equation (18), for $j = 3$, the proof of Lemma 4.1 requires to establish the asymptotic behavior of $c_{mn|_\Sigma}$, $R^{(3)}_{mn|_\Sigma}$, and $r^{(3)}_{mn|_\Sigma}$.

i. First, we have (see Equation (33) in [4]):

$$c_{mn|_\Sigma} \sim -\mathrm{i} e_\Gamma \sigma k a_\Gamma + e_\Gamma; \quad \text{as} \quad k a_\Gamma \to +\infty \tag{24}$$

ii. Next, we know that (see Chapter 4 p. 30 in [9]):

$$R^{(3)}_{mn|_\Sigma} \sim h^{(1)}_n(\sigma k a_\Gamma) \tag{25}$$

where $h^{(1)}_n$ denotes the spherical Hankel function of the first kind (also called spherical Bessel function of the third kind, see Chapter 10 in [1]). In addition, we have (see p. 437 in [1]):

$$h^{(1)}_n(\sigma k a_\Gamma) = \sqrt{\frac{\pi}{2\sigma k a_\Gamma}} H^{(1)}_{n+1/2}(\sigma k a_\Gamma) \tag{26}$$

where $H^{(1)}_{n+1/2}$ denotes the Hankel function of the first kind and of order $n + 1/2$ (see [1], p. 355).
Hence, for $n \sim \sigma k a_\Gamma$, it follows from Equations (25) and (26) that:

$$R^{(3)}_{m\sigma k a_\Gamma|_\Sigma} \sim \sqrt{\frac{\pi}{2\sigma k a_\Gamma}} H^{(1)}_{\sigma k a_\Gamma}(\sigma k a_\Gamma); \quad \text{as} \quad k a_\Gamma \to +\infty \tag{27}$$

On the other hand, we know that (see (9.3.31) and (9.3.32) p. 368 in [1]):

$$H^{(1)}_{\sigma k a_\Gamma}(\sigma k a_\Gamma) \sim \frac{2^{1/3}(1-\mathrm{i}\sqrt{3})}{3^{2/3}\Gamma(2/3)(\sigma k a_\Gamma)^{1/3}}; \quad \text{as} \quad k a_\Gamma \to \infty \tag{28}$$

Hence it follows from substituting Equation (28) into Equation (27) that:

$$R^{(3)}_{m\sigma k a_{\Gamma|\Sigma}} \sim \frac{\pi^{1/2}2^{5/6}\exp(-\mathrm{i}\pi/3)}{3^{2/3}\Gamma(2/3)}\frac{1}{(\sigma k a_\Gamma)^{5/6}}; \text{ as } k a_\Gamma \to +\infty \tag{29}$$

iii. Last, we derive the asymptotic behavior of $r^{(3)}_{mn|_\Sigma}$ given by Equation (6). Observe that, (see (4.1.16) p. 32 in [9]):

$$r^{(3)}_{mn|_\Sigma} = \frac{R^{(3)'}_{mn|_\Sigma}}{R^{(3)}_{mn|_\Sigma}} \sim e_\Gamma \sigma k a_\Gamma \frac{h^{(1)'}_n(\sigma k a_\Gamma)}{h^{(1)}_n(\sigma k a_\Gamma)}; \text{ as } k a_\Gamma \to +\infty \tag{30}$$

where the $h^{(1)'}_n$ is the derivative of the spherical Hankel function of the first kind (see Chapter 10 in [1]). In addition, we have (see (10.1.1) p. 437 in [1]):

$$\frac{h^{(1)'}_n(\sigma k a_\Gamma)}{h^{(1)}_n(\sigma k a_\Gamma)} \sim \frac{H^{(1)'}_{n+1/2}(\sigma k a_\Gamma)}{H^{(1)}_{n+1/2}(\sigma k a_\Gamma)} - \frac{1}{2\sigma k a_\Gamma}; \text{ as } k a_\Gamma \to +\infty \tag{31}$$

where $H^{(1)'}_{n+1/2}$ denotes the derivative of the Hankel function of the first kind and of order $n+1/2$ (see [1], Chapter 9 & 10).
Hence, for $n \sim \sigma k a_\Gamma$, it follows (see (9.3.5) p. 366 or (9.3.31)–(9.3.34) p. 368 in [1]) that:

$$\frac{H^{(1)'}_{\sigma k a_\Gamma}(\sigma k a_\Gamma)}{H^{(1)}_{\sigma k a_\Gamma}(\sigma k a_\Gamma)} \sim \frac{2^{1/3}3^{1/3}\Gamma(2/3)e_\Gamma}{\Gamma(1/3)(\sigma k a_\Gamma)^{1/3}}\exp(2\mathrm{i}\pi/3); \text{ as } k a_\Gamma \to +\infty \tag{32}$$

Consequently, we deduce from Equations (30)–(32), that:

$$r^{(3)}_{m\sigma k a_{\Gamma|\Sigma}} \sim \frac{2^{1/3}3^{1/3}\Gamma(2/3)e_\Gamma\exp(\mathrm{i}2\pi/3)}{\Gamma(1/3)}(\sigma k a_\Gamma)^{2/3}; \text{ as } k a_\Gamma \to +\infty \tag{33}$$

The substitution of Equations (24), (29), and (33) into Equation (18) concludes the proof of Lemma 4.1.

The next result states the behavior of the Wronskian-like operator $W^{3,4}_{mn}(\Gamma,\Sigma)$, given by Equation (20), for the high-order modes.

Lemma 4.2 *For all* $(m,n) \in \mathbb{N}^2$ *such that* $n \sim \sigma k a_\Gamma$ *and* $m \leq n$*, the Wronskian-like function* $W^{3,4}_{mn}(\Gamma,\Sigma)$ *satisfies:*

$$W^{3,4}_{m\sigma k a_\Gamma}(\Gamma,\Sigma) \sim -\frac{\pi^{1/2} 2^{5/6} e_\Gamma \sigma^{1/6} \exp\left(\frac{2}{3}\sigma k a_\Gamma \zeta^{3/2}\right)}{3^{2/3}(\sigma^2-1)^{1/4}\Gamma(2/3)(k a_\Gamma)^{5/6}};\ \text{as}\ k a_\Gamma \to \infty \quad (34)$$

where the variable ζ *is given by Equation (22).*

Proof of Lemma 4.2 It follows from the expression of $W^{3,4}_{mn}(\Gamma,\Sigma)$ given by Equation (20), that the proof of Lemma 4.2 requires the derivation of the asymptotic behavior of both $R^{(j)}_{mn_{|\Gamma}}$ and $\Psi^{(j)}_{mn|_\Sigma}$ for $j = 3,\ 4$.

i. The asymptotic behavior of the radial spheroidal wave functions $R^{(j)}_{mn_{|\Gamma}}$ $(j = 3,\ 4)$ is given by (see Chapter 4 p. 30 in [9]):

$$R^{(j)}_{mn_{|\Gamma}} \sim h^{(j-2)}_{n_{|\Gamma}};\quad \text{as}\quad k a_\Gamma \to \infty \quad (35)$$

where $h^{(2)}_{n_{|\Gamma}}$ denotes the spherical Hankel function of the second kind of order n (see Chapter 10 in [1]). On the other hand, we know that (see p. 437 in [1]):

$$h^{(2)}_{n_{|\Gamma}} = \sqrt{\frac{\pi}{2\sigma k a_\Gamma}} H^{(2)}_{n+1/2}(k a_\Gamma) \quad (36)$$

where $H^{(2)}_{n+1/2}$ denotes the Hankel function of the second kind and of order $n + 1/2$ (see Chapter 9 & 10 in [1]). In addition, for $n \sim \sigma k a_\Gamma$ and as $k a_\Gamma \to \infty$, we know that for $j = 3,\ 4$ we have (see (9.3.31)–(9.3.34) p. 368 in [1]):

$$H^{(j)}_{\sigma k a_\Gamma}(k a_\Gamma) \sim \left(\frac{4\zeta}{(1-\sigma^{-2})}\right)^{1/4} \frac{\mathrm{Ai}\left((\sigma k a_\Gamma)^{2/3}\zeta\right) + (-1)^j \mathrm{iBi}\left((\sigma k a_\Gamma)^{2/3}\zeta\right)}{(\sigma k a_\Gamma)^{1/3}} \quad (37)$$

where Ai and Bi are the Airy functions (see p. 446 in [1]), and ζ is defined by Equation (22).

Moreover, we have (see Equation (10.4.9) p. 446 in [1]):

$$\mathrm{Ai}(z) \mp \mathrm{iBi}(z) = 2\exp(\mp \mathrm{i}\pi/3)\mathrm{Ai}\left(z\exp(\pm \mathrm{i}2\pi/3)\right) \quad (38)$$

where $z = (\sigma k a_\Gamma)^{2/3}\zeta$.

On the other hand, the asymptotic behavior of the Airy function is given by (see (10.4.59) p. 448 in [1]):

$$\mathrm{Ai}(z) \sim \frac{\pi^{-1/2}}{2} z^{-1/4} \exp\left(-\frac{2}{3}z^{3/2}\right);\quad \text{as}\quad k a_\Gamma \to \infty \quad (39)$$

where this time $z = (\sigma k a_\Gamma)^{2/3}\zeta \exp(\pm \mathrm{i}2\pi/3)$.
Hence, as $ka_\Gamma \to \infty$, it follows from Equations (35)–(39), that:

$$R^{(3)}_{m\sigma k a_{\Gamma|\Sigma}}(ka_\Gamma) = \overline{R^{(4)}_{m\sigma k a_{\Gamma|\Sigma}}(ka_\Gamma)} \sim \frac{-\mathrm{i}}{(\sigma^2-1)^{1/4} k a_\Gamma} \exp\left(-\frac{2}{3}\sigma k a_\Gamma \zeta^{3/2}\right) \quad (40)$$

ii. The asymptotic behavior of $\Psi^{(4)}_{m\sigma k a_{\Gamma|\Sigma}}$ is an immediate consequence of the asymptotic behavior of $\Psi^{(3)}_{mn|_\Sigma}$ obtained in Lemma 4.1 and the fact that (see (21.9.2) and (21.9.3), p. 756 in [1]):

$$R^{(4)}_{m\sigma k a_{\Gamma|\Sigma}} = \overline{R^{(3)}_{m\sigma k a_{\Gamma|\Sigma}}}; \quad \text{as} \quad ka_\Gamma \to +\infty$$

and

$$r^{(4)}_{m\sigma k a_{\Gamma|\Sigma}} \sim \overline{r^{(3)}_{m\sigma k a_{\Gamma|\Sigma}}}; \quad \text{as} \quad ka_\Gamma \to +\infty \quad (41)$$

together with the asymptotic behavior of $c_{mn|_\Sigma}$ given by Equation (24). Hence, we have:

$$\Psi^{(4)}_{m\sigma k a_{\Gamma|\Sigma}} \sim \frac{\pi^{1/2} 2^{5/6} e_\Gamma \exp(-\mathrm{i}\pi/6)}{3^{2/3}\Gamma(2/3)} (\sigma k a_\Gamma)^{1/6}; \text{ as } ka_\Gamma \to +\infty \quad (42)$$

iii. Last, the proof of Lemma 4.2 results from substituting Equations (23), (40), and (42) into Equation (20).

Last, we establish the asymptotic behavior of the radial spheroidal wave function of the first kind.

Lemma 4.3 *For all $(m,n) \in \mathbb{N}^2$ such that $n \sim \sigma k a_\Gamma$ and $m \leq n$, the function $R^{(1)}_{mn|_\Gamma}$ satisfies:*

$$R^{(1)}_{mn|_\Gamma} \sim \frac{\exp\left(-\frac{2}{3}\sigma k a_\Gamma \zeta^{3/2}\right)}{2(\sigma^2-1)^{1/4} k a_\Gamma}; \quad \text{as} \quad ka_\Gamma \to +\infty \quad (43)$$

where ζ is given by Equation (22).

Proof of Lemma 4.3 First, observe that the asymptotic behavior of $R^{(1)}_{mn|_\Gamma}$, as $ka_\Gamma \to +\infty$, is given by (see Chapter 4 p. 30 in [9]):

$$R^{(1)}_{mn|_\Gamma} \sim j_n(ka_\Gamma) \quad (44)$$

where j_n denotes the spherical Bessel function of the first kind (see Chapter 10 in [1]). In addition, we have (see p. 437 in [1]):

$$j_n(ka_\Gamma) = \sqrt{\frac{\pi}{2ka_\Gamma}} J_{n+1/2}(ka_\Gamma) \quad (45)$$

where $J_{n+1/2}$ denotes the Bessel function of order $n + 1/2$ (see Chapters 9 & 10 in [1]).

Hence, it follows from Equations (44)–(45) that:

$$R^{(1)}_{mn|_\Gamma} \sim \sqrt{\frac{\pi}{2ka_\Gamma}} J_{n+1/2}(ka_\Gamma); \quad \text{as} \quad ka_\Gamma \to +\infty \tag{46}$$

On the other hand, for $n \sim \sigma ka_\Gamma$, we also have (see (9.3.6) p. 366 in [1]):

$$J_{\sigma ka_\Sigma}(ka_\Sigma) \sim \left(\frac{4\zeta}{1-\frac{1}{\sigma^2}}\right)^{1/4} \frac{\text{Ai}\left((\sigma ka_\Sigma)^{2/3}\zeta\right)}{(\sigma ka_\Sigma)^{1/3}}; \text{ as } ka_\Gamma \to \infty \tag{47}$$

where ζ is given by Equation (22) and Ai is the Airy function (whose asymptotic behavior is given by (see (10.4.59), p. 448 in [1]):

$$\text{Ai}\left((\sigma ka_\Gamma)^{2/3}\zeta\right) \sim \frac{\pi^{-1/2}}{2}\left[(\sigma ka_\Gamma)^{2/3}\zeta\right]^{-1/4} \exp\left(-\frac{2}{3}(\sigma ka_\Gamma)\zeta^{3/2}\right) \tag{48}$$

Hence, as $ka_\Gamma \to \infty$, it follows from Equations (47) and (48) that:

$$J_{\sigma ka_\Sigma}(ka_\Sigma) \sim \left(\frac{4}{1-\frac{1}{\sigma^2}}\right)^{1/4} \frac{\pi^{-1/2}}{2(\sigma ka_\Gamma)^{1/2}} \exp\left(-\frac{2}{3}(\sigma ka_\Gamma)\zeta^{3/2}\right) \tag{49}$$

Finally, substituting Equation (49) into Equation (46) leads to:

$$R^{(1)}_{m\sigma ka_{\Gamma|_\Gamma}} \sim \frac{\exp\left(-\frac{2}{3}\sigma ka_\Gamma \zeta^{3/2}\right)}{2(\sigma^2-1)^{1/4} ka_\Gamma}; \quad \text{as} \quad ka_\Gamma \to +\infty$$

which concludes the proof of Lemma 4.3.

We are now ready to prove Theorem 3.1.

Proof of Theorem 3.1

From Lemmas 4.1–4.3 and the definition of the Fourier coefficient τ^{DtN}_{mn} (see Equation (17)) that for all $(m,n) \in \mathbb{N}^2$ such that $n \sim \sigma ka_\Gamma$ and $m \le n$, we deduce that:

$$\tau^{\text{DtN}}_{m\sigma ka_\Gamma} \sim -\frac{\exp(-\text{i}5\pi/6) d^{\text{inc}}_{m\sigma ka_\Gamma}}{2} \exp\left(-\frac{4}{3}\sigma ka_\Gamma \zeta^{3/2}\right); \text{ as } ka_\Gamma \to \infty \tag{50}$$

where $d^{\text{inc}}_{m\sigma ka_\Gamma}$ is given by Equation (10) and the real number ζ is given by Equation (22).

On the other hand, we know that the Fourier coefficient d^{inc}_{mn} corresponding to the incident plane wave satisfies (see Lemma 5.1 p. 247 in [17] or Lemma 3.13 p. 594 in [4]):

$$\left|d^{\text{inc}}_{mn}\right| < 4\kappa \left(\frac{\sqrt{e_\Gamma ka_\Gamma}}{\pi}\right)^{1/4}; \quad \text{as} \quad ka_\Gamma \to \infty \tag{51}$$

where $\kappa \approx 1.086435$ (see (22.14.17), p. 787 in [1]).

The substitution of Equation (51) into Equation (50) leads to the desired result, and therefore concludes the proof of Theorem 3.1.

5. SUMMARY AND CONCLUSION

We have investigated analytically the asymptotic behavior of the reflected high-order modes induced by the presence of the so-called DtN2 absorbing boundary condition when employed for solving exterior Helmholtz problems with prolate spheroid shaped scatterers. We proved that, contrary to the situation when the second-order Balyliss-Gunzburger-Turkel condition (BGT2) is used, these spurious modes decay exponentially in the high frequency regime. This result proves the effectiveness of the DtN2 boundary condition when employed for solving high-frequency acoustic scattering problems by elongated scatterers. It also demonstrates the superiority of the DtN2 condition over the widely used BGT2 boundary condition. Given that, this study suggests that DtN2 absorbing boundary condition is the primary candidate to be employed for solving high frequency scattering problems by elongated scatterers.

ACKNOWLEDGMENT

The authors acknowledge the support by INRIA/CSUN Associate Team Program, by ANR/AHPI research program (Agence Nationale de la Recherche/Analyse Harmonique et Problèmes Inverses) and by the Aquitaine/Euskadi research program. Any opinions, findings, conclusions or recommendations expressed in this material are those of the authors and do not necessarily reflect the views of ANR, BCAM, CSUN, or INRIA.

APPENDIX A. CLASSIFICATION OF THE MODES

A very brief classification of the prolate spheroidal modes u_{mn} is presented in this section. More details can be found in Annexe D in [17]. The proposed classification has the advantage to coincide with the standard classification of the spherical modes when the eccentricity of the prolate tends to 1, that is, the prolate spheroid tend to become a sphere. Recall that the spherical modes u_n ($n \in \mathbb{N}$) are categorized into three groups: (a) propagating modes when $n < ka_\Sigma$, evanescent modes for $n > ka_\Sigma$, and grazing modes in the limit case where $n \approx ka_\Sigma$ [19].

Definition A.1 *For all $(m, n) \in \mathbb{N}^2$ such that $m \leq n$, the prolate spheroidal mode u_{mn} is said to be:*

i. a propagating mode if $(u_{mn})^{-1}\frac{\partial}{\partial\xi}(\sinh\xi\frac{\partial u_{mn}}{\partial\xi})$ *is negative,*

ii. an evanescent mode if $(u_{mn})^{-1}\frac{\partial}{\partial\xi}(\sinh\xi\frac{\partial u_{mn}}{\partial\xi})$ *is positive,*

iii. a grazing mode if $\frac{\partial}{\partial\xi}(\sinh\xi\frac{\partial u_{mn}}{\partial\xi})$ *is zero.*

The next result states a preliminary characterization of the classification introduced in Definition A.1.

Proposition A.2 *Assume the exterior Boundary* Σ *to be located at* $\xi=\xi_1$*. Then, for all* $(m,n)\in\mathbb{N}^2$ *such that* $m\leq n$*, the prolate spheroidal mode* u_{mn} *is said to be:*

i. a propagating mode if $\lambda_{mn|_\Sigma}\ll(kf)^2\cosh^2\xi_1-\frac{m^2}{\sinh^2\xi_1}$,

ii. an evanescent mode if $\lambda_{mn|_\Sigma}\gg(kf)^2\cosh^2\xi_1-\frac{m^2}{\sinh^2\xi_1}$,

iii. a grazing mode if $\lambda_{mn|_\Sigma}\approx(kf)^2\cosh^2\xi_1-\frac{m^2}{\sinh^2\xi_1}$,

where $\lambda_{mn|_\Sigma}$ *is the prolate spheroidal eigenvalue associated to the* (mn)*th mode (see p. 11 in [9]), and* f *is the interfocal distance of the prolate spheroid whose surface is* Σ*.*

Proof of Proposition A.2 First, we apply the Helmholtz operator to the mode u_{mn} (see (B.118) p. 287 in [17]). Hence, we have:

$$\frac{1}{\sinh\xi}\frac{\partial}{\partial\xi}\left(\sinh\xi\frac{\partial u_{mn}}{\partial\xi}\right)=\left(\lambda_{mn}-(kf)^2\cosh^2\xi+\frac{m^2}{\sinh^2\xi}\right)u_{mn}\quad\text{(A1)}$$

Then, the proof of Proposition A.2 is an immediate consequence of substituting

$$f=\sqrt{a_\Sigma^2-b_\Sigma^2}=a_\Sigma\cosh\xi_1^{-1}\quad\text{(A2)}$$

and

$$e_\Sigma=\frac{1}{\cosh\xi_1}\quad\text{(A3)}$$

into Equation (A1), and then applying Definition A.1.

Consequently, in the high-frequency regime ($ka_\Gamma\to+\infty$), Proposition (A.2) can be formulated as follows.

Corollary A.3 *Assume the exterior Boundary* Σ *to be located at* $\xi=\xi_1$ *and* $ka_\Gamma\to+\infty$*. Then, for all* $(m,n)\in\mathbb{N}^2$ *such that* $m\leq n$*, the prolate spheroidal mode* u_{mn} *is said to be:*

i. a propagating mode if $n-m\ll\frac{ka_\Sigma}{2e_\Sigma}$,

ii. an evanescent mode if $n-m\gg\frac{ka_\Sigma}{2e_\Sigma}$,

iii. a grazing mode if $n-m\approx\frac{ka_\Sigma}{2e_\Sigma}$.

Proof of Corollary A.3 First, we observe that (see Equation (21.7.6), p. 754 in [1]) that when $ka_\Gamma \to +\infty$ (and therefore $ka_\Sigma \to +\infty$), we have:

$$\lambda_{mn|_\Sigma} \sim (2n - 2m + 1)e_\Sigma ka_\Sigma \tag{A4}$$

Hence, it follows from substituting Equations (A2)–(A3) into Equation (A4), that:

$$-\lambda_{mn|_\Sigma} + (kf)^2 \cosh^2 \xi_1 - \frac{m^2}{\sinh^2 \xi_1} \approx 0; \quad \text{as} \quad ka_\Gamma \to +\infty$$

which can be re-written as follow:

$$-(2n-2m+1)e_\Sigma ka_\Sigma + (e_\Sigma ka_\Sigma)^2 \cosh^2 \xi_1 - \frac{m^2}{\sinh^2 \xi_1} \approx 0; \text{ as } ka_\Gamma \to +\infty$$

Using Equation (A3) and the fact that $e_\Sigma ka_\Sigma \neq 0$, we deduce that:

$$n - m \approx \frac{\mathbf{ka}_\Sigma}{2\mathbf{e}_\Sigma} - \frac{m^2}{2e_\Sigma ka_\Sigma \sinh^2 \xi_1} - \frac{1}{2}$$

Corollary A.3 is then a consequence of retaining the high-order terms (in bold) of the previous approximation.

Remark A.4 *In the particular situation where $a_\Sigma = \sigma a_\Gamma$, the classification of the modes given by Corollary A.3 can be formulated in more convenient way as follows:*

Assume the exterior Boundary Σ to be located at $\xi = \xi_1$ and $ka_\Gamma \to +\infty$. Then, for all $(m, n) \in \mathbb{N}^2$ such that $m \leq n$, the prolate spheroidal mode u_{mn} is said to be:

i. a propagating mode if $n - m \ll \frac{\sigma ka_\Gamma}{2e_\Gamma}$,

ii. an evanescent mode if $n - m \gg \frac{\sigma ka_\Gamma}{2e_\Gamma}$,

iii. a grazing mode if $n - m \approx \frac{\sigma ka_\Gamma}{2e_\Gamma}$.

This classification seems to be more convenient for easily identifying, in the high frequency regime, the type of modes that are absorbed or not by the DtN2 absorbing boundary condition, as well as for comparing with the behavior of the modes induced by the standard BGT2 absorbing boundary condition.

Remark A.5 *Observe that it follows from Theorem (4) and Remark (A.4) that, for the modes such that $n \sim \sigma ka_\Gamma$, all three categories of modes decay exponentially, and therefore are absorbed very quickly. To better identify such modes, one need to consider two cases depending on the value of the eccentricity e_Σ $(= e_\Gamma)$ of the prolate spheroidal-shaped exterior boundary Σ. More specifically, assume the exterior boundary Σ to be located at $\xi = \xi_1$, $ka_\Gamma \to +\infty$, and $(m, n) \in \mathbb{N}^2$ such that $n \sim \sigma ka_\Gamma$ with $m \leq n$. Then, we have:*

a. For $e_\Sigma = e_\Gamma \in (0, 5)$, corresponding to a moderately elongated scatterer, the mode u_{mn} is said to be a propagating for any m such that $0 \leq m \leq n$ as $m \gg (1 - \frac{1}{2e_\Gamma})\sigma k a_\Gamma$.

b. If $e_\Sigma = e_\Gamma \in [0.5, 1)$, corresponding to an elongated scatterer, the mode u_{mn} is said to be:

i. a propagating mode if $\sigma k a_\Gamma \geq m \gg (1 - \frac{1}{2e_\Gamma})\sigma k a_\Gamma$,

ii. an evanescent mode if $0 \leq m \ll (1 - \frac{1}{2e_\Gamma})\sigma k a_\Gamma$,

iii. a grazing mode if $m \approx (1 - \frac{1}{2e_\Gamma})\sigma k a_\Gamma$.

REFERENCES

1. Abramovitz, M. and I. Stegun, *Handbook of Mathematical Functions with Formulas, Graphs and Mathematical Tables*, Dover Publications, New York, 1972.
2. Antoine, X., M. Darbas, and Y. Y. Lu, "An improved surface radiation condition for high frequency acoustic scattering problems," *Computer Methods in Applied Mechanics and Engineering*, Vol. 195, Nos. 33–36, 4060–4074, 2006.
3. Barucq, H., R. Djellouli, and A. Saint-Guirons, "Performance assessment of a new class of local absorbing boundary conditions for elliptical-shaped boundaries," *Applied Numerical Mathematics*, Vol. 59, 1467–1498, 2009.
4. Barucq, H., R. Djellouli, and A. Saint-Guirons, "High frequency analysis of the efficiency of a local approximate DtN2 boundary condition for prolate spheroidal-shaped boundaries," *Wave Motion*, Vol. 8, No. 47, 583–600, 2010.
5. Bayliss, A., M. Gunzburger, and E. Turkel, "Boundary conditions for the numerical solution of elliptic equations in exterior regions," *SIAM J. Appl. Math.*, Vol. 42, No. 2, 430–451, 1982.
6. Bowman, J. J., T. B. A. Senior, and P. L. E. Uslenghi, *Electromagnetic and Acoustic Scattering by Simple Shapes*, North-Holland Publishing Company, Amsterdam, 1969.
7. Colton, D. and R. Kress, *Integral Equations in Scattering Theory, Pure and Applied Mathematics*, John Wiley and Sons, New York, 1983.
8. Darbas, M., "Prconditionneurs analytiques de type Calderon pour les formulations intgrales de problmes de diffraction d'ondes," Thèse de Doctorat, Universités de Toulouse 1 et Toulouse 3, INSA Toulouse, France, 2004.
9. Flammer, C., *Spheroidal Wave Functions*, Standford University Press, Standford, CA, 1957.

10. Givoli, D. and J. B. Keller, "Nonreflecting boundary conditions for elastic waves," *Wave Motion*, Vol. 12, No. 3, 261–279, 1990.
11. Harari, I. and R. Djellouli, "Analytical study of the effect of wave number on the performance of local absorbing boundary conditions for acoustic scattering," *Applied Numerical Mathematics*, Vol. 50, 15–47, 2004.
12. Harari, I. and T. J. R. Hughes, "Analysis of continuous formulations underlying the computation of time-harmonic acoustics in exterior domains," *Comput. Methods Appl. Mech. Engrg.*, Vol. 97, No. 1, 103–124, 1992.
13. Kriegsmann, G. A., A. Taflove, and K. R. Umashankar, "A new formulation of electromagnetic wave scattering using an on-surface radiation boundary condition approach," *IEEE Trans. Antennas and Propagation*, Vol. 35, No. 2, 153–161, 1987.
14. Nigsch, M., "Numerical studies of time-independent and time-dependent scattering by several elliptical cylinders," *Journal of Computational and Applied Mathematics*, Vol. 204, 231–241, 2007.
15. Reiner, R. C., R. Djellouli, and I. Harari, "The performance of local absorbing boundary conditions for acoustic scattering from elliptical shapes," *Comput. Methods Appl. Mech. Engrg.*, Vol. 195, 3622–3665, 2006.
16. Reiner, R. C. and R. Djellouli, "Improvement of the performance of the BGT2 condition for low frequency acoustic scattering problems," *Wave Motion*, Vol. 43, 406–424, 2006.
17. Saint-Guirons, A.-G., "Construction et analyse de conditions absorbantes de type Dirichlet-to-Neumann pour des frontières ellipsoïdales," Thèse de Doctorat, Université de Pau et des Pays de l'Adour, France, 2008. Available online at: http://tel.archives-ouvertes.fr.
18. Stratton, J. A., *Electromagnetic Theory*, McGraw-Hill, New York, 1941.
19. Taylor, M. E., *Pseudodifferential Operators*, Princeton University Press, Princeton, New Jersey, 1981.
20. Turkel, E., "Boundary conditions and iterative schemes for the helmholtz equation in unbounded regions," *Computational Methods for Acoustics Problems*, 127–158, F. Magoulès (ed.), Saxe-Coburg Publications, 2009.